Surface-Based Seeding for Blood Flow Exploration

Benjamin Köhler[1], Mathias Neugebauer[1], Rocco Gasteiger[1], Gábor Janiga[2], Oliver Speck[3], Bernhard Preim[1]

[1]Department of Simulation and Graphics, University of Magdeburg
[2]Department of Fluid Dynamics and Thermodynamics, University of Magdeburg
[3]Department of Biomedical Magnetic Resonance, University of Magdeburg
benjamin.koehler@st.ovgu.de

Abstract. Qualitative visual analysis of flow patterns in cerebral aneurysms is important for assessing the risk of rupture. According to current research, the flow patterns close to the aneurysm surface (e.g. impingement zone) provide a good insight. Streamlines can be easily interpreted and are commonly used for visualizing and exploring blood flow. However, standard ways of seeding these streamlines, e.g. manually oriented planes, are not suitable for explicit exploration of local near-wall flow. In this work, we introduce a novel surface-based seeding strategy. Our approach is flexibly applicable to measured as well as simulated data, so we present results for both. Informal domain expert feedback confirmed the suitability of our method to explore near-wall blood flow. The intuitive interaction scheme and the ease of use were appreciated.

1 Introduction

Cerebral aneurysms are a serious health risk for patients. A rupture can cause a subarachnoid hemorrhage with a high fatality rate [1]. Thus, a reliable risk assessment is of major interest. Since experiences have shown that small aneurysms rupture as well, risk assessment by considering only their size or shape is not sufficient. Recent researches [2] pointed out that hemodynamics play an important role for the risk assessment of aneurysms and vascular diseases in general. Since a relation between risk of rupture and complex flow patterns close to the surface is indicated, not only the velocity but also the characteristic of the blood flow is important. Thus, a local, visual analysis of the flow, e.g. at the aneurysm dome, is essential.

In order to qualitatively estimate the flow complexity, adequate flow visualization is necessary. Streamlines can be easily interpreted and are commonly used for visualizing and exploring blood flow [3]. In this work, we want to focus on the seeding of these streamlines. Existing approaches often use centerlines and let the user move an orthogonal plane along the direction of the centerlines [4]. Different seeding patterns are provided by specific probability distributions on the plane. The centerline extraction works well for vessels but

T. Tolxdorff et al. (Hrsg.), *Bildverarbeitung für die Medizin 2012,* Informatik aktuell,
DOI 10.1007/978-3-642-28502-8_16,

often is error-prone in aneurysms due to their shape. Hence, free plane placement correction without assistance is provided. This includes the tedious task of repeated rotation and translation of the plane as well as the necessity for frequent viewport changes. More sophisticated approaches [5] additionally guide the interaction using the aneurysms ostium and provide elaborate exploration widgets, but demand a complex anatomical analysis as prerequisite.

In this work, we introduce a surface-based seeding strategy for streamlines with an intuitive interaction scheme that allows a qualitative analysis of the blood flow especially near vessel boundaries.

2 Material and methods

2.1 Data

There are basically two ways to obtain flow data: direct measurement using 4D PC-MRI or computational fluid dynamics (CDF) simulations [1]. Measured data can be obtained relatively fast and represent the in-vivo flow situation, but can contain image artifacts and noise. Also it is not available in every case. CFD provides a detailed, smooth and noise-free flow representation. Simulating the flow before and after treatment (stenting/coiling) is also possible. However, the accuracy of the flow directly depends on the choice of model assumptions and boundary conditions.

Our first dataset contains three saccular aneurysms and was directly measured using a 4D PC-MRI. Our second dataset contains a basilar aneurysm with distinct satellites and was simulated using CFD. Our approach requires a mesh representation of the surface. This can be obtained by segmenting the vessels using a threshold-based method, removing artifacts by applying a connected component analysis and finally using marching cubes to reconstruct the triangles. Remeshing is applied to gain a mesh quality sufficient for CFD. Given this surface mesh and a vector field of the flow, our approach is generally applicable on simulated and measured data.

2.2 Seeding positions

The principal idea is to select an area directly on the triangular surface, extrude every vertex along a certain vector, connect each triangle to its extruded version (Fig. 1a) and then generate random positions within these prisms. Assuming that a prism with the vertices $p_i, i = 0..5$ is convex, random positions p_{random} within can easily be generated using barycentric coordinates with random weights $w_i \in [0, 1]$

$$p_{\text{random}} = \sum_{i=0}^{5} w_i \cdot p_i \quad \text{with} \sum_{i=0}^{5} w_i = 1 \tag{1}$$

So, the question is how to choose the extrusion vectors. Using the negated normals does not provide a limitation for the maximally allowed translation. If

Fig. 1. Triangle extrusion (left) and extrusion along $\boldsymbol{x}$ (right)

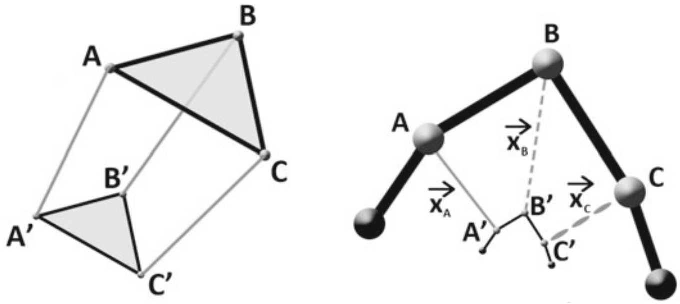

the vertices are moved too far, the prisms degenerate and this causes errors in the barycentric interpolation due to the concavity.

Shrinking of the mesh is usually an unwanted side effect of standard laplacian smoothing. However, we take advantage of this effect and repeatedly apply it until the surface has only about 5% of its original area left. Fig. 2 shows the mesh of our simulated dataset before (a) and after (b) laplacian smoothing. Our (not normalized) extrusion vector $\boldsymbol{x}$ is the difference $p_\Delta - p_{\text{orig}}$ with p_{orig} as the original vertex and p_Δ as the same vertex after shrinking the mesh. An extruded vertex $p_{\boldsymbol{x}}$ is only allowed to lie between p_{orig} and p_Δ

$$p_{\boldsymbol{x}} = p_{\text{orig}} + t \cdot \boldsymbol{x} \quad \text{with } t \in [0, 1] \tag{2}$$

Since laplacian smoothing repeatedly replaces every vertex with the average of its direct neighborhood, the problem of degenerating prisms will not occur, illustrated by Fig. 1b.

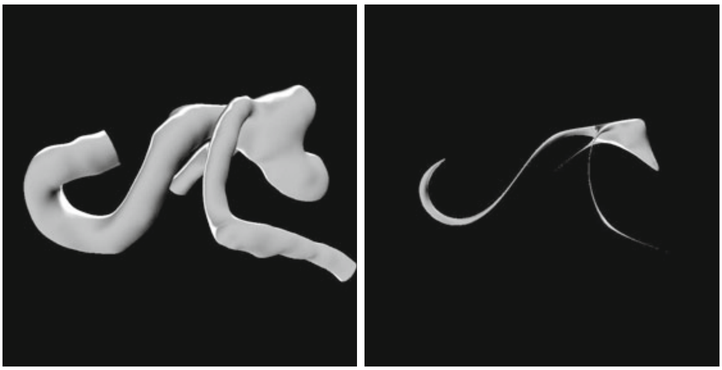

Fig. 2. Full-size (left) and shrunken (right) meshes

2.3 Interaction scheme

The mouse-based interaction consists of three tasks. First, a point on the surface has to be selected by clicking the left mouse button. Secondly, the size of the selection may be adjusted using the mouse wheel. It grows uniformly in every direction using an advancing front algorithm. The resulting selection of a surface patch can also be transformed into a ring-shaped selection, which is suitable for exploring flow in vessels. The initial patch selection consists of inner vertices and one connected boundary. A uniform growing is simulated until the boundary splits into two parts. This happens when the growing selection merges. Now, the shortest path between the two boundaries is determined. Then, the path to the original selection is retraced and every vertex along this path(s) is added to the selection. Fig. 3a shows the initial selection and the result after closing the ring. Finally, the selection has to be extruded. This is achieved by holding the right mouse button and then moving the mouse up or down which changes $t \in [0, 1]$ (Chpt. 2.2). Fig. 3b and c illustrate a ring and a cap selection for different t-values.

3 Results and discussion

We proposed a surface-based seeding strategy with an intuitive interaction scheme that improves the exploration of the blood flow and helps to understand its characteristic. Given a surface mesh and a vector field of the flow, our method is generally applicable on simulated as well as measured data.

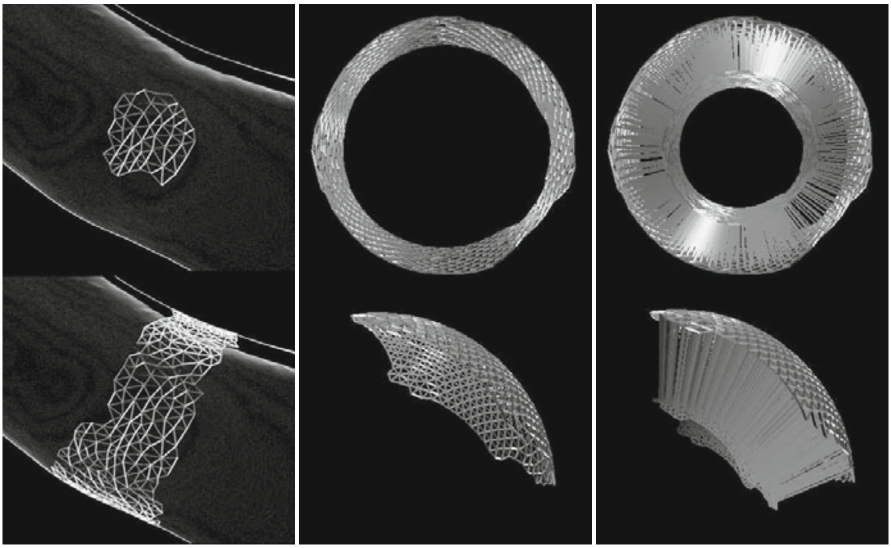

(a) Ring selection (b) Extrusion with $t = 0$ (c) Extrusion with $t = 0.4$

Fig. 3. Visualization of a vessel

We applied our method to the two datasets described in Sect. 2.1. Fig. 4 and 5 show several selections in the upper and resulting streamlines in the lower rows for the simulated and the measured dataset. Fig. 4a illustrates a cap selection on a basilar aneurysm with distinct satellites and Fig. 4b shows a ring selection on a vessel (Chpt. 2.3). The resulting streamlines are vortex-structured and indicate a complex blood flow characteristic. Parallel to this, Fig. 5a and b show flow behavior in/near saccular aneurysms using a cap selection on an aneurysm (a) and a ring selection on a vessel (b). The streamlines in Fig. 5b visualize the blood flowing partially into the aneurysm showing a swirling behavior and partially following the vessels course. The t-parameter for the extrusion was set to 0.2 in all cases.

A domain expert, who is familiar with Ensight, was asked to interact with the datasets. He seeded only a few streamlines at once with a short integration time, which allowed him to understand the flow characteristics near the boundaries

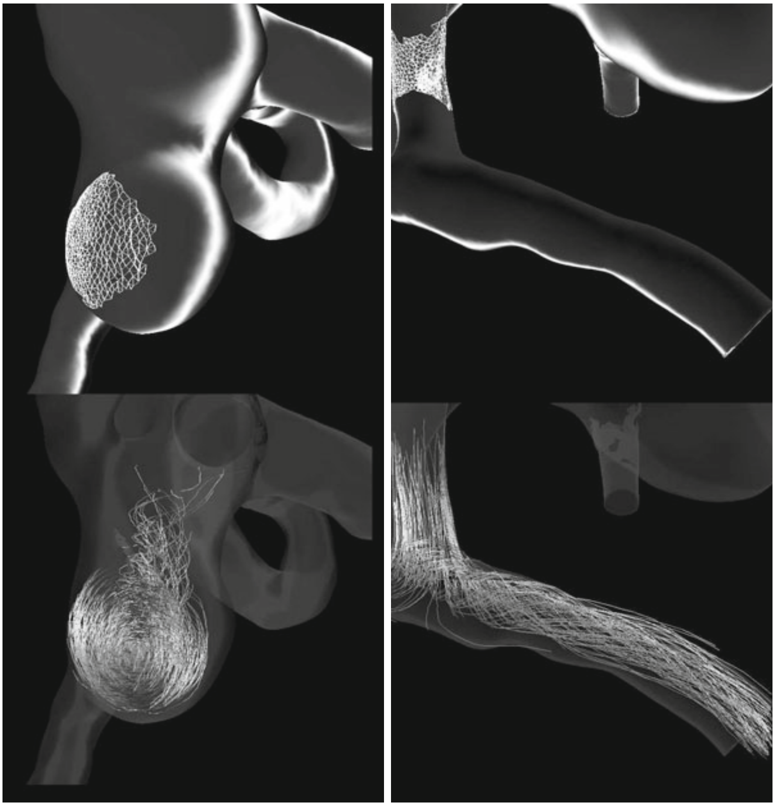

(a) Cap selection, basilar aneurysm (b) Ring selection on vessel

Fig. 4. Simulated dataset

easily. The suitability of our approach was confirmed and the ease of use was appreciated.

References

1. Gasteiger R, Janiga G, Stucht D, et al. Vergleich zwischen 7 Tesla 4D PC-MRI-Flussmessung und CFD-Simulation. In: Proc BVM; 2011. p. 304–8.
2. Cebral JR, Mut F, Weir J, et al. Association of hemodynamic characteristics and cerebral aneurysm rupture. AJNR Am J Neuroradiol. 2011;32(2):264–70.
3. Salzbrunn T, Jänicke H, Wischgoll T, et al. The state of the art in flow visualization: partition-based techniques. In: SimVis; 2008. p. 75–92.
4. van Pelt R, Olivan Bescos J, Breeuwer M, et al. Exploration of 4D MRI blood flow using stylistic visualization. IEEE Trans Vis Comput Graph. 2010;16:1339–47.
5. Neugebauer M, Janiga G, Beuing O, et al. Anatomy-guided multi-level exploration of blood flow in cerebral aneurysms. Comput Graph Forum. 2011;30(3):1041–50.

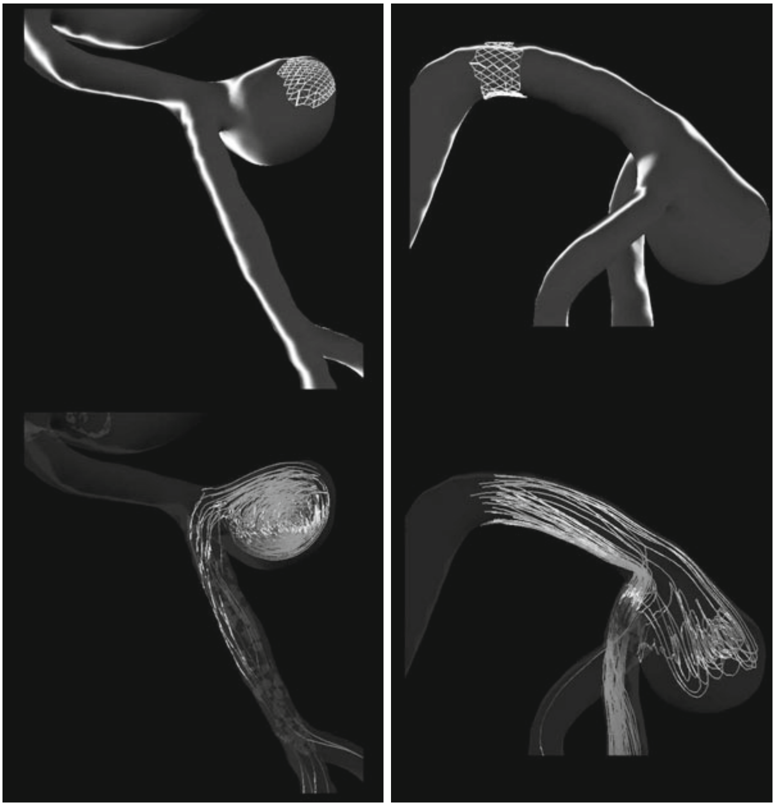

(a) Cap selection, saccular aneurysm (b) Ring selection on vessel

Fig. 5. Measured dataset